Computer Assisted Mechanics and Engineering Sciences, 5: 389–398, 1998.

On suction driven flow and heat transfer in a pipe filled with porous media

Oluwole Daniel Makinde
Applied Mathematics Department, University of North, Private Bag X1106, Sovenga 0727, South Africa

Precious Sibanda
Department of Mathematics, University of Zimbabwe, PO Box MP 167, Mt. Pleasant, Harare, Zimbabwe

(Received October 21, 1997)

The axisymmetric flow of a viscous fluid and heat transfer in a pipe filled with porous media driven by suction at the pipe wall is examined. For low suction Reynolds number flow, asymptotic solutions are developed. Using MAPLE, the solution series is extended and a bifurcation study is performed. Our results show that a decrease in the permeability of porous media may reduce the magnitude of heat transfer across the wall. The absence of real solutions of the given type between two turning points is also noticed and this gap of no solution disappears as the permeability of the porous media decreases.

1. Introduction

Flow in a pipe filled with a porous media under the influence of uniform wall suction is important for the following reasons. Firstly, the study is of immediate relevance to a multitude of technological applications, e.g. in lubrication of porous bearings, ground water hydrology and in industrial filtration processes where a porous matrix is used inside the fluid passage. Several geophysical and energy engineering applications were elaborated by Kim *et al.* [8]. Secondly, nutritional problems in the alimentary canal such as indigestion, constipation, diarrhea, etc., could be effectively rectified if the biomechanics of chyme absorption in the small intensine (which can be easily simulated using this model) is well understood.

Berman [1] presented an exact solution of the Navier-Stokes equations that describe the steady flow in a channel driven by suction at the walls. He exploited the Hiemenz [7] similarity form of solution in order to reduce the problem to a fourth order nonlinear ordinary differential equation. In this regard numerous authors e.g. Terrill and Thomas [12], Durlovsky and Brady [4], Zaturska and Banks [14], Makinde [9], etc., have developed and generalized this exact solution for the case flow in a pipe driven by uniform wall suction. The most amazing and significant result in their study is the presence of a region bounded by two turning points in the solution field where no real solution of the given type exist.

However, in the present work, the suction driven flow in a pipe filled with porous media is considered. In this type of study, the common approach has been to use Darcy's law in the porous medium (generally with low permeabilities) together with the Navier-Stokes equations.

Our objective is to study the effect of porous media on the bifurcation that takes place in the flow field as the suction Reynolds number increases. To achieve this goal, we have employed a novel computational approach to the study of bifurcations presented by Drazin and Tourigny [5]. The technique relies on the use of power series in the bifurcation parameter for a particular

solution branch. This technique was utilized by Makinde [10] in the study of steady flow in a slightly asymmetrical channel.

In Secs. 2 and 3, we establish the mathematical formulation for the problem. The computer extension of the resulting perturbation series solution, its analysis and analytic continuation, including bifurcation study are examined in Sec. 4. We discuss the pertinent findings in Sec. 5.

2. Mathematical formulation

We consider the flow of viscous incompressible fluid in a pipe of circular cross-section filled with a porous media. Take a cylindrical polar coordinate system (r, θ, z) where Oz lies along the centre of the pipe, r is the distance measured radially and θ is the azimuthal angle. Let u and v be the velocity components in the directions of z and r increasing respectively, a the pipe characteristic radius, V the characteristic suction (negative for injection) velocity and K a parameter that characterizes permeability of the porous media. Then, for axisymmetric steady viscous incompressible flow, the Navier-Stokes equations are

$$u\frac{\partial u}{\partial z} + v\frac{\partial u}{\partial r} = -\frac{1}{\rho}\frac{\partial p}{\partial z} + \nu\nabla^2 u - \frac{\nu}{K}u, \tag{1}$$

$$u\frac{\partial v}{\partial z} + v\frac{\partial v}{\partial r} = -\frac{1}{\rho}\frac{\partial p}{\partial r} + \nu\left(\nabla^2 v - \frac{v}{r^2}\right) - \frac{\nu}{K}v, \tag{2}$$

$$u\frac{\partial T}{\partial z} + v\frac{\partial T}{\partial r} = \alpha\nabla^2 T, \tag{3}$$

where $\nabla^2 = \partial^2/\partial r^2 + \partial/r\partial r + \partial^2/\partial z^2$, p is the pressure, T the temperature, ρ the density, α the thermal diffusivity and ν the kinematic viscosity of the fluid. The equation of continuity is

$$\frac{\partial}{\partial r}(rv) + r\frac{\partial u}{\partial z} = 0. \tag{4}$$

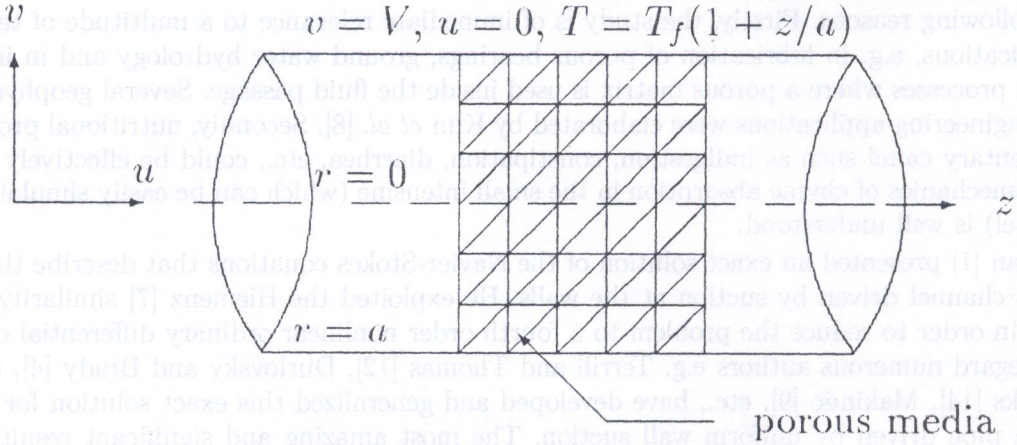

Fig. 1. Schematic diagram of the problem

The appropriate boundary equations are

$$\frac{\partial u}{\partial r} = 0, \quad \frac{\partial T}{\partial r} = 0, \quad v = 0 \quad \text{on } r = 0, \tag{5}$$

$$u = 0, \quad v = V, \quad T = T_f\left(1 + \frac{z}{a}\right) \quad \text{on } r = a, \tag{6}$$

where T_f is the reference temperature. We shall introduce the stream-function Ψ and vorticity ω in the following manner:

$$u = \frac{1}{r}\frac{\partial \Psi}{\partial r} \quad \text{and} \quad v = -\frac{1}{r}\frac{\partial \Psi}{\partial z}, \tag{7}$$

$$\omega = \frac{\partial v}{\partial z} - \frac{\partial u}{\partial r} = -\frac{1}{r}\frac{\partial^2 \Psi}{r \partial z^2} - \frac{1}{r}\frac{\partial^2 \Psi}{\partial r^2} + \frac{1}{r^2}\frac{\partial \Psi}{\partial r}. \tag{8}$$

Eliminating the pressure p from (1) and (2) by using (7) and (8) we get

$$\frac{1}{r}\frac{\partial(\Psi, \omega)}{\partial(r, z)} + \frac{\omega}{r^2}\frac{\partial \Psi}{\partial z} + \frac{\nu}{K}\omega = \nu\left[\nabla^2 \omega - \frac{\omega}{r^2}\right], \tag{9}$$

and

$$\frac{1}{r}\frac{\partial(\Psi, T)}{\partial(r, z)} = \alpha \nabla^2 T. \tag{10}$$

The following dimensionless variables are introduced;

$$\overline{\omega} = \frac{a\omega}{V}, \qquad \overline{z} = \frac{z}{a}, \qquad \overline{r} = \frac{r}{a}, \qquad \overline{\Psi} = \frac{\Psi}{Va^2}, \qquad \overline{T} = \frac{T}{T_f} - 1. \tag{11}$$

And we seek a similarity form of solution due to Hiemenz [7], (neglecting the bars for clarity), that is,

$$\Psi = zF(r), \qquad \omega = -zG(r), \qquad T = z\theta(r). \tag{12}$$

The dimensionless form of the governing equations together with the boundary conditions in terms of similarity variables F and G, can be written as

$$\frac{d}{dr}\left[\frac{1}{r}\frac{d}{dr}(rG)\right] = R\left[\frac{G}{r}\frac{dF}{dr} - F\frac{d}{dr}\left(\frac{G}{r}\right) + \sigma G\right], \tag{13}$$

$$\frac{d}{dr}\left(r\frac{d\theta}{dr}\right) = QR\left[\theta\frac{dF}{dr} - F\frac{d\theta}{dr}\right], \tag{14}$$

$$G = \frac{d}{r}\left(\frac{1}{r}\frac{dF}{dr}\right). \tag{15}$$

The boundary conditions are

$$\frac{d}{dr}\left(\frac{1}{r}\frac{dF}{dr}\right) = 0, \quad F = 0, \quad \frac{d\theta}{dr} = 0 \quad \text{on } r = 0, \tag{16}$$

$$\frac{dF}{dr} = 0, \quad F = -1, \quad \theta = 1 \quad \text{on } r = 1. \tag{17}$$

Hence the problem depends on three principal parameters, i.e., the porosity parameter $\sigma = (a\nu/KV)$, the Prandtl number $Q = \nu/\alpha$ and the suction Reynolds number $R(= Va/\nu)$.

3. METHOD OF SOLUTION

To solve equations (13)–(17), it is convenient to take a power series expansion in the suction Reynolds number R, i.e.

$$F = \sum_{i=0}^{\infty} R^i F_i, \qquad G = \sum_{i=0}^{\infty} R^i G_i, \qquad \theta = \sum_{i=0}^{\infty} R^i \theta_i. \tag{18}$$

Substituting the above expressions (18) into (13)–(17) and collecting the coefficients of like powers of R, we obtain the following;

Zeroth Order:

$$\frac{d}{dr}\left[\frac{1}{r}\frac{d}{dr}(rG_0)\right] = 0, \qquad G_0 = \frac{d}{dr}\left(\frac{1}{r}\frac{dF_0}{dr}\right), \qquad \frac{d}{dr}\left[r\frac{d\theta_0}{dr}\right] = 0, \tag{19}$$

$$F_0 = 0, \qquad \frac{d}{dr}\left(\frac{1}{r}\frac{dF_0}{dr}\right) = 0, \qquad \frac{d\theta_0}{dr} = 0 \quad \text{on } r = 0, \tag{20}$$

$$F_0 = -1, \qquad \frac{dF_0}{dr} = 0, \qquad \theta_0 = 0 \quad \text{on } r = 1. \tag{21}$$

Higher Order ($n \geq 1$):

$$\frac{d}{dr}\left[\frac{d}{dr}(rG_n)\right] = R\sum_{i=0}^{n-1}\left[\frac{G_i}{r}\left(\frac{dF_{n-i-1}}{dr}\right) - F_i\frac{d}{dr}\left(\frac{G_{n-i-1}}{r}\right) + \sigma G\right], \tag{22}$$

$$G_n = \frac{d}{dr}\left(\frac{1}{r}\frac{dF_n}{dr}\right), \qquad \frac{d}{dr}\left[r\frac{d\theta_n}{dr}\right] = QR\sum_{i=0}^{n-1}\left[\theta_i\frac{dF_{n-i-1}}{dr} - F_i\frac{d\theta_{n-i-1}}{dr}\right], \tag{23}$$

$$F_n = 0, \qquad \frac{d}{dr}\left(\frac{1}{r}\frac{dF_n}{dr}\right) = 0, \qquad \frac{d\theta_n}{dr} = 0 \quad \text{on } r = 0, \tag{24}$$

$$F_n = 0, \qquad \frac{dF_n}{dr} = 0, \qquad \theta_n = 0 \quad \text{on } r = 1. \tag{25}$$

We have written a MAPLE program that calculates successively the coefficients of the solution series. In outline, it consists of the following segments:

(1) Declare arrays for the solution series coefficients e.g., F = arrays(0..43), G = array(0..43), θ = array(0..43), etc.

(2) Input the leading order terms and their derivatives, i.e. F_0, G_0, θ_0, etc.

(3) Compute the skin friction, axial pressure gradient, centerline axial velocity and wall heat transfer coefficients.

Details of the MAPLE program are given in the Appendix. Some of the solutions for the stream-function, vorticity and temperature are given by

$$\begin{aligned} F(r) = {} & r^4 - 2r^2 + \frac{1}{72}r^2(r^2-1)^2(2r^2+3\sigma-8)R \\ & + \frac{1}{86400}r^2-1)^2(16r^6+120r^4\sigma-208r^4-460r^2\sigma+75r^2\sigma^2 \\ & + 768r^2+1360\sigma-150\sigma^2-2656)R^2+..., \end{aligned} \tag{26}$$

$$G(r) = 8r + \frac{1}{3}r(4r^4 - 12r^2 + 3r^2\sigma - 2\sigma + 6)R \tag{27}$$

$$+\frac{1}{2160}r(48r^8 + 240r^6\sigma - 480r^6 + 1440r^4 - 840r^4\sigma + 90r^4\sigma^2$$

$$+1440r^2\sigma - 2640r^2 - 636\sigma + 75\sigma^2 + 1216)R^2 + ...,$$

$$\theta(r) = 1 + RQ(r^2 - 1)(r^2 - 3) + \frac{1}{288}R^2Q(r^2 - 1)(r^6 - 8Qr^4 - 7r^4) \tag{28}$$

$$+ \frac{1}{288}R^2Q(r^2 - 1)(2r^4\sigma + 46Qr^2 - 4r^2\sigma + 11r^2)$$

$$- \frac{1}{288}R^2Q(r^2 - 1)(170Q + 2\sigma - 5) + ...$$

The non-dimensional skin friction is given by

$$t_w = -\frac{\mu V}{a}\beta \quad \text{on} \quad r = 1, \tag{29}$$

where $\beta = G(1)$ and we have,

$$\beta = 8 + \frac{1}{3}(-2 + \sigma)R - \frac{1}{2160}(416 - 204\sigma + 15\sigma^2)R^2 + ..., \tag{30}$$

where μ is the dynamic coefficient of viscosity. From the axial component of the Navier-Stokes equations, the pressure drop in the longitudinal direction can be obtained. Thus, in dimensionless form we have

$$\frac{\partial p}{\partial z} = zH = z\left\{\frac{1}{r}\frac{d}{dr}\left[r\frac{d}{dr}\left(\frac{1}{r}\frac{dF}{dr}\right)\right] - \frac{R}{r}\left[\frac{1}{r}\left(\frac{dF}{dr}\right)^2 - F\frac{d}{dr}\left(\frac{1}{r}\frac{dF}{dr}\right) + \sigma\frac{dF}{dr}\right]\right\}, \tag{31}$$

and we obtain the dimensionless fluid pressure $\overline{p}$ as

$$p = \frac{z^2}{2}\left\{8 + \left(-12 + \frac{8\sigma}{3}\right)R + \left(-\frac{88}{135} + \frac{3\sigma}{10} - \frac{\sigma^2}{72}\right)R^2 + ...\right\}, \tag{32}$$

where the bar has been dropped for consistency and $\overline{p}$ is scaled with ($\overline{p} = ap/\mu V$). The rate of heat transfer at the wall given as $S = d\theta/dr$ at $r = 1$ can easily be obtained as

$$S = -RQ - \frac{11}{12}R^2Q^2 + \frac{1}{2160}R^3Q^2(24\sigma - 1593Q - 58) + ... \tag{33}$$

4. Computer extension and bifurcation study

In order to investigate the flow structure at moderately large suction Reynolds numbers using the series summation techniques, we expand the following in powers of suction Reynolds number; $\beta = -G(1)$, $\gamma = u(0)$, $H = \partial p/z\partial z$ and $S = d\theta/dr$ at $r = 1$, representing the skin friction, the centrline axial velocity, the axial pressure gradient and the rate of wall heat transfer respectively. For a given value of Prandtl number Q, we have obtained the series for several values of $\sigma \geq 0$, for instance, the expansion when $Q = 7.0$ (i.e water) and $\sigma = 0.1$ is

$$\beta = 8 - \frac{19}{30}R - \frac{1583}{8640}R^2 - \frac{1600673}{30240000}R^3 - \frac{1202094983}{74649600000}R^4 + ..., \tag{34}$$

$$\gamma = -4 - \frac{77}{360}R - \frac{1681}{28800}R^2 - \frac{1043809397}{60963840000}R^3 + ..., \tag{35}$$

$$H = 8 - \frac{176}{15}R - \frac{2687}{28800}R^2 - \frac{8466539}{45360000}R^3 - \frac{5080262107}{87091200000}R^4 + ..., \tag{36}$$

$$S = -7R - \frac{539}{12}R^2 - \frac{2745617}{10800}R^3 - \frac{2936585869}{2073600}R^4 + ... \quad \text{as} \quad R \to 0. \tag{37}$$

The first 65 coefficients for the series represented above were obtained. We observe that for very large permeability of the porous media i.e. as $\sigma \to 0$, the signs of the coefficients are the same and are monotonically decreasing in magnitude, hence the convergence of the series may be limited by a singularity on the positive real axis. The Domb-Sykes plot [3] together with Neville's [11] extrapolation at $1/n = 0$, (i.e. $n \to \infty$) reveal that the radius of convergence depends on the porosity parameter i.e. $R_c = R_c(\sigma)$ and for the case $\sigma = 0.1$ represented by the above series, we obtain $R_c = 2.336$.

The effect of a porous media on heat transfer across the wall is also investigated. It is observed that a decrease in the permeability of the porous media may reduce the magnitude of heat transfer across the wall (see Table 1).

Table 1. Variation of wall heat transfer with respect to σ

R	$\lvert S\rvert, \sigma = 0$	$\lvert S\rvert, \sigma = .01$	$\lvert S\rvert, \sigma = 0.3$	$\lvert S\rvert, \sigma = 0.5$
0.1	1.7173628	1.7171037	1.7165864	1.7160701
0.2	27.55573	27.530516	27.480209	27.430088
0.3	613.33869	612.51637	610.87689	609.24424
0.4	7976.4460	7964.7670	7971.4849	7918.3037

Meanwhile, following Drazin and Tourigny [5], we examine the bifurcation in the flow field using the series solutions obtained for several values of σ. The procedure leads to a special type of Hermite-Padé approximant. Let us suppose that the partial sum

$$U_N(\lambda) = \sum_{n=1}^{N} a_n \lambda^n = U(\lambda) + O(\lambda^{N+1}) \quad \text{as} \quad \lambda \to 0, \tag{38}$$

is a known solution. We shall make the simplest hypothesis in the context of nonlinear problems by assuming that $U(\lambda)$ is the local representation of an algebraic function u of λ. Therefore, we seek a polynomial $F_d = F_d(\lambda, u)$ of degree $d \geq 2$, i.e.,

$$F_d(\lambda, u) = \sum_{m=1}^{d} \sum_{k=0}^{m} f_{m-k} k^{\lambda^{m-k}} u^k, \tag{39}$$

such that

$$\frac{\partial F_d}{\partial u}(0,0) = 1, \tag{40}$$

$$F_d(\lambda, U_n(\lambda)) = O(\lambda^{N+1}) \quad \text{as} \quad \lambda \to 0. \tag{41}$$

Condition (40), which yields $f_{0,1} = 1$, ensures that the polynomila F_d has only one root which vanishes at $\lambda = 0$ and also normalizes F_d. There are thus

$$1 + \sum_{m=2}^{d} (m+1) = \frac{1}{2}(d^2 + 3d - 2), \tag{42}$$

undetermined coefficient in the polynomial (39). The requirement (41) reduces the problem to a system of N linear equations for the unknown coefficients of F_d. The entries of the underlying matrix depend only on the N given coefficients a_n. Henceforth, we shall take

$$N = \frac{1}{2}(d^2 + 3d - 2), \tag{43}$$

so that the number of equations equals the number of unknowns. A bifurcation occurs where the solutions of the nonlinear system change their qualitative character as a parameter changes. In particular, bifurcation theory is about how the number of steady solutions of a system depends on a Newton's diagram (Vainberg and Trenogin, [13]). Using the above procedure, we consider first the case of $\sigma = 0$ which coincides with the Berman [1] problem. Our results show the presence of two disconnected turning points R_1 and R_2. We also noticed that

$$\beta \sim \beta_{-1} R^{-1}, \qquad H \sim H_{-1} R^{-1}, \qquad \gamma \sim \gamma_{-1} R^{-1} \quad \text{as} \quad R \to 0, \tag{44}$$

on the secondary branch (see Table 3 and Table 4 below). This is also in agreement with the computed results of Terril and Thomas [12] and Makinde [9]. Secondly, we investigate the effect of porous media on the flow bifurcation diagram. Our results show that the radius of convergence R_1, increase with an increase in porosity parameter or decrease in the permeability of the porous media. As $\sigma \to \infty$, this turning point eventually disappears (see Table 2).

Table 2. Computations showing variation of bifurcation point with respect to porosity parameter σ

σ	0	0.1	0.5	1.0	1.5	2.0	2.5	3.0
R_1	2.298	2.336	2.505	2.766	3.114	3.616	4.461	11.149

5. Results and discussion

We are interested in the combined effects of wall suction and permeability of the porous media on the flow characteristics. It is interesting to note that $\sigma = 0$ gives the case of a pipe without any porous media inside the fluid passage way. As $\sigma \to \infty$ the permeability of the porous media inside the pipe decreases. From our numerical calculations in Tables 1–2, we observe that the rate of heat transfer across the pipe wall decreases with a decrease in the permeability of the porous media. At very large permeability, we observe the presence of two turning points in the solution field between which no real solution of the assumed type exists. This region disappears as the permeability of the porous media reduces. Figures and show sketches of the bifurcation diagram and wall heat transfer respectively.

Finally, most filtration devices are of low permeability. Consequently, the magnitude of the skin friction will automatically increase in order to maintain constant suction (Fig. 2b). This may eventually damage the equipment. Hence, for efficient industrial filtration process, it is recommended that such devices are made to withstand the friction.

Table 3. Computations of bifurcation points using the D-T method ($\sigma = 0$)

d	N	$R_1^{(d)}$	$R_2^{(2)}$
2	4	2.219858965302754653007841	...
3	8	2.299591435888679094512663	...
4	13	2.298944554015399102282373	9.231445938
5	19	2.298947597198399236964974	9.112409713
6	26	2.298947597447284940827505	9.112481962
7	34	2.298947597447332260530929	9.112503439
8	43	2.298947597447332263107502	9.112502909
9	53	2.298947597447332263107410	9.112502849
10	64	2.298947597447332263107410	9.112502849

Table 4. Computations showing asymptotic behaviour of secondary solution branch as $R \to 0$ using the D-T method ($\sigma = 0$)

d	N	$R_{-1}^{(d)}$	$\gamma_{-1}^{(d)}$	$H_{-1}^{(d)}$
2	4	...	...	...
3	4	−73.19132206	−34.64246021419	...
4	13	−67.43240223	−35.66324435704	−346.37931680
5	19	−67.49732198	−35.31456772558	−348.17295010
6	26	−67.66383415	−35.31497742406	−348.64827877
7	34	−67.67015929	−35.31497341348	−348.65065895
8	43	−67.67020677	−35.31497346667	−348.65071000
9	53	−67.67020667	−35.31497346683	−348.65071000
10	64	−67.67020667	−35.31497346683	−348.65071000

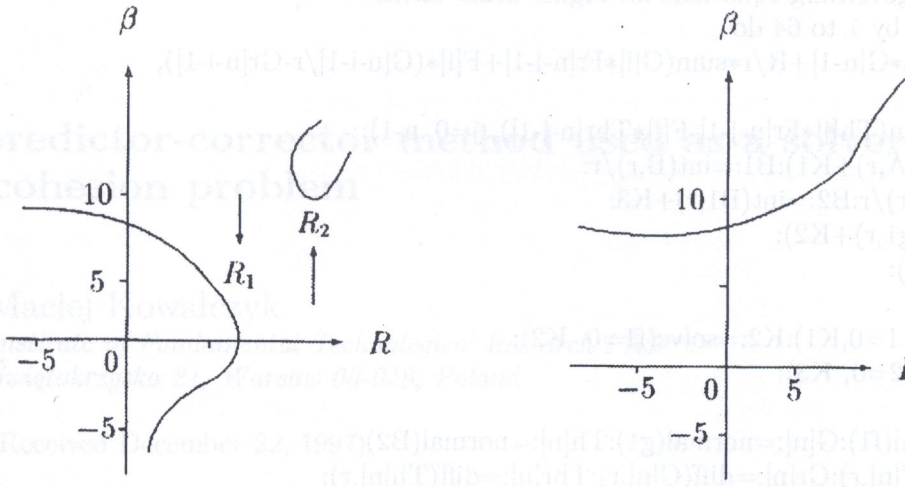

(a) High permeability ($\sigma \to 0$) (b) Low permeability ($\sigma \to \infty$)

Fig. 2. A sketch of the bifurcation diagram in the (R, β)- plane

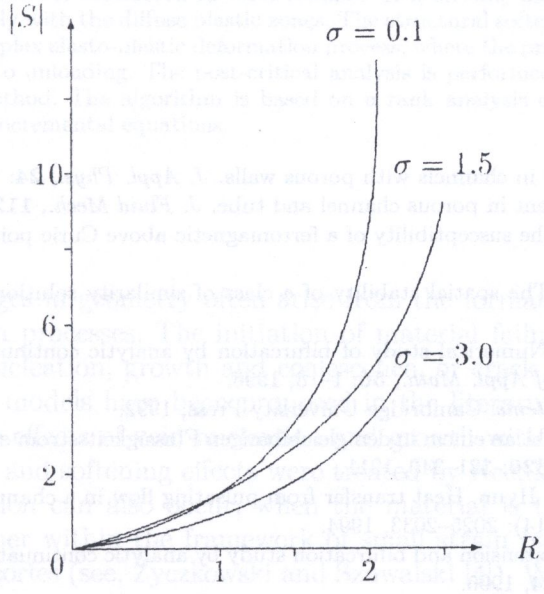

Fig. 3. The rate of heat transfer at the wall, $Q = 0.7$

6. Appendix

The MAPLE procedure to silve the system of equations (20)–(23) and the values of the coefficients of wall shear stress.

- Decleration of arrays for the solution series coefficients Digits: =50:
  F:=array(0. .64):G:=array(0. . 64):Fr:=array(0. . 64):
  Gr:=array(0. . 64):Th:=array(0. . 64): Thr:=array(0. . 64):

- Input the leading order terms and their derivatives
  F[0]:=(r^4 − 2∗r^2):G[0]:=8∗r:Th[0]:=1:
  Fr[0]:=diff(F[0],r):Gr[0]:=diff(G[0],r):Thr[0]:=diff(Th[0],r):

- Solving the governing equations for higher order terms
  for n from 1 by 1 to 64 do
  A:=R*sigma*G[n-1]+R/r*sum(G[i]*Fr[n-i-1]+F[i]*(G[n-i-1]/r-Gr[n-i-1]),
  i=0,..n-1):
  B:=R*Q*sum(Th[j]*Fr[n-j-1]-F[j]*Thr[n-j-1]), j=0..n-1):
  g11:=r*(int(A,r)+K1):B1:=int(B,r)/r:
  g1:=int(g11,r)/r:B2:=int(B1,r)+K3:
  f11:=r*(int(g1,r)+K2):
  f1:=int(f11,r):
  r:=1:
  K1:=solve(f11=0,K1):K2:=solve(f1=0, K2):
  K3:=solve(B2=0, K3):
  r:='r':
  F[n]:=normal(f1):G[n]:=normal(g1):Th[n]:=normal(B2):
  Fr[n]:=diff(F[n],r):Gr[n]:=diff(G[n],r):Thr[n]:=diff(Th[n],r):
  K1:='K1':K2:='K2':K3:='K3':

- Computing the skin friction coefficients (e.g sigma=0.1)
  print(evalf(sub(r=1,G[n])));
  od:
  quit();

References

[1] A.S. Berman. Laminar flow in channels with porous walls. *J. Appl. Phys.*, **24**: 1232–1235, 1953.

[2] J.F. Brady. Flow development in porous channel and tube. *J. Fluid Mech.*, **112**: 127–150, 1984.

[3] C. Domb, M.F. Sykes. On the susceptibility of a ferromagnetic above Curie point. *Proc. R. Soc. Lond., Ser. A.*, **240**: 214–228, 1957.

[4] L. Durlovsky, J.F. Brady. The spatial stability of a class of similarity solutions. *Phys. Fluids*, **27**: 1068–1076, 1984.

[5] P.G. Drazin, Y. Tourigny. Numerical study of bifurcation by analytic continuation of a function defined by a power series. *SIAM Jour. of Appl. Math.*, **56**: 1–18, 1996.

[6] P.G. Drazin. *Nonlinear Systems.* Cambridge University Press, 1992.

[7] K. Hiemenz. Die Grenzschicht an einem in den gleichfomigen Flussigkeitsstrom eingetauchten geraden Kreiszylinder. *Dinglers Polytech. J.*, **326**: 321–340, 1911.

[8] S.Y. Kim, B.H. Kang, J.M. Hyun. Heat transfer from pulsating flow in a channel filled with porous media. *Int. J. Heat mass Transfer*, **37**(14): 2025–2033, 1994.

[9] O.D. Makinde. Computer extension and bifurcation study by analytic continuation of porous tube flow problem. *J. Math. Phys. Sc.*, **30**: 1–24, 1996.

[10] O.D. Makinde. Steady flow in a linearly diverging asymetrical channel. *CAMES.*, **4**(2): 157–165, 1997.

[11] E.H. Neville. Iterative interpolation. *J. Indian Math. Soc.*, **20**: 87–120, 1934.

[12] R.M. Terrill, P.W. Thomas. Laminar flow through a uniformly porous pipe. *Appl. Sci. Res.*. **21**: 37–67, 1969.

[13] M.m. Vainberg, V.A. Trenogin. Theory of branching of solutions of nonlinear equations. *Noordoff, Leyden*, 1974.

[14] M.B. Zaturska, W.H.H. Banks. Flow in a pipe driven by suction at an accelerating wall. *Acta Mechanica*, **110**: 111–121, 1995.